



On the low-order character of coherence resonance in the midlatitude wind-driven ocean circulation



Stefano Pierini

Dipartimento di Scienze per l'Ambiente
Università di Napoli Parthenope - Napoli (Italy)
stefano.pierini@uniparthenope.it

In an excitable autonomous dynamical system, self-sustained relaxation oscillations (ROs) usually emerge past a homoclinic bifurcation (when a control parameter μ , e.g. the forcing amplitude, exceeds a given threshold μ_0 , a "tipping point"). ROs can however be excited *also* for $\mu < \mu_0$ provided the system is perturbed by a suitable noise (a phenomenon known as "coherence resonance", CR). Three main questions arise:

- What kind of noise is required for CR to occur?
- How sensitive is the activation of CR to the distance $\mu - \mu_0$ from the bifurcation?
- If ROs are actually observed in a real system, which of the two alternatives is most likely to occur? (this point was recently analyzed by Ditlevsen and Johnsen, 2010, in the context of Dansgaard-Oeschger events).

This problem was studied by Pierini (2010) with reference to the bimodal decadal ROs of the Kuroshio Extension. These were revealed by altimetric observations by Qiu and Chen (2005) and were simulated numerically by Pierini (2006) and Pierini et al. (2009).

In order to analyze the low-order character of this phenomenon, a highly truncated spectral QG ocean model was recently developed and applied to the same problem by Pierini (2011). In this poster we summarize the main results concerning CR and a method (denoted as "phase selection") proposed to analyze the excitation mechanism. The intrinsic low-frequency variability found in the corresponding autonomous system is discussed in another poster of the same author in session NP3.1.

REFERENCES

Ditlevsen, P. D., and S. J. Johnsen, 2010: Tipping points: early warning and wishful thinking. *Geophys. Res. Lett.*, **37**, L19703, doi:10.1029/2010GL044486.
Pierini, S., 2006: A Kuroshio Extension System model study: decadal chaotic self-sustained oscillations. *J. Phys. Oceanogr.*, **36**, 1605-1625.
Pierini, S., 2010: Coherence resonance in a double-gyre model of the Kuroshio Extension. *J. Phys. Oceanogr.*, **40**, 238-248.
Pierini, S., 2011: Low-frequency variability, coherence resonance and phase selection in a low-order model of the wind-driven ocean circulation. *J. Phys. Oceanogr.*, **41**, in press.
Pierini, S., H. A. Dijkstra, and A. Riccio, 2009: A nonlinear theory of the Kuroshio Extension bimodality. *J. Phys. Oceanogr.*, **39**, 2212-2229.
Qiu, B., and S. Chen, 2005: Variability of the Kuroshio Extension jet, recirculation gyre, and mesoscale eddies on decadal time scales. *J. Phys. Oceanogr.*, **35**, 2090-2103.

The low-order ocean model

The model is based on the evolution equation of potential vorticity in the QG reduced-gravity approximation:

$$\frac{\partial}{\partial t} (\nabla_\lambda^2 \psi - F\psi) + \gamma J(\psi, \nabla_\lambda^2 \psi) + \psi_x = -R\nabla_\lambda^2 \psi - T\tau_y$$

The truncated spectral model is obtained by expanding the streamfunction ψ as:

$$\psi(\mathbf{x}, t) = \sum_{i=1}^4 \Psi_i(t) |i\rangle$$

$$\begin{aligned} |1\rangle &= e^{-\alpha x} \sin x \sin y & |3\rangle &= e^{-\alpha x} \sin 2x \sin y \\ |2\rangle &= e^{-\alpha x} \sin x \sin 2y & |4\rangle &= e^{-\alpha x} \sin 2x \sin 2y \end{aligned}$$

The system reduces to a set of four coupled nonlinear ODEs:

$$\begin{aligned} \dot{\Psi}_1 + p\Psi_1 + q\Psi_3 + N_1 &= W_1 \\ \dot{\Psi}_2 + u\Psi_2 + v\Psi_4 + N_2 &= W_2 \\ \dot{\Psi}_3 + m\Psi_3 + o\Psi_1 + N_3 &= W_3 \\ \dot{\Psi}_4 + s\Psi_4 + t\Psi_2 + N_4 &= W_4 \end{aligned}$$

The nonlinear terms N_i are given by

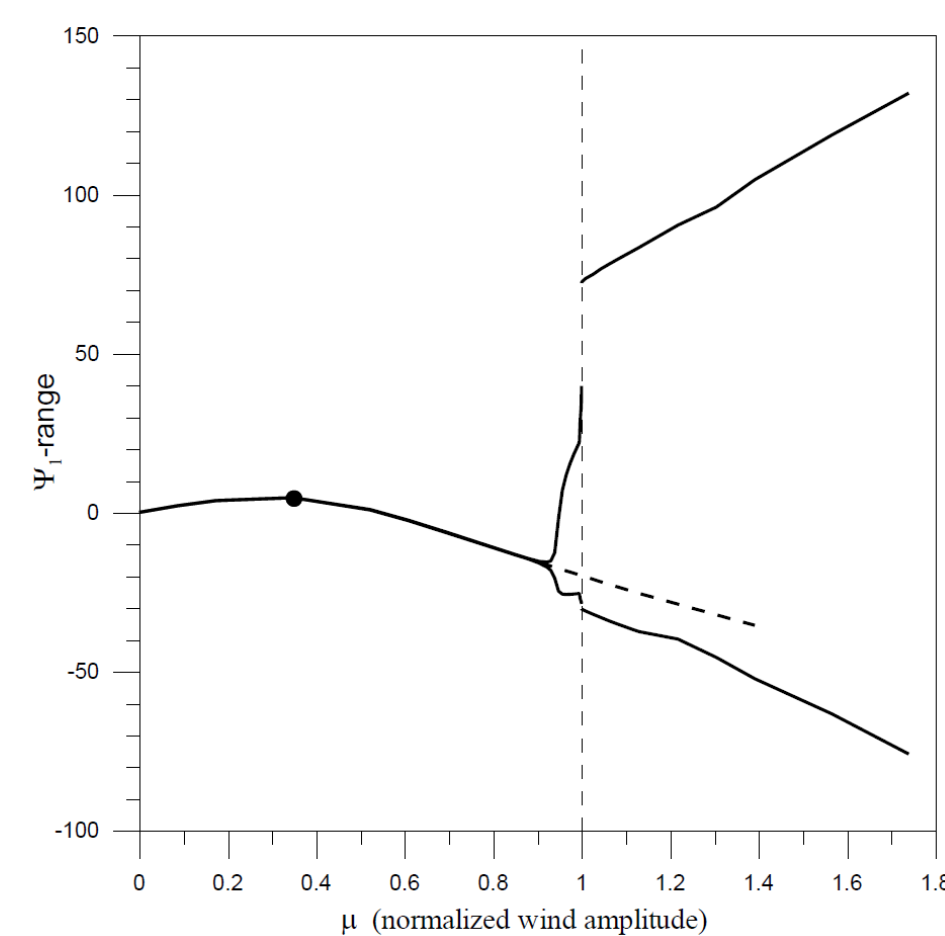
$$N_i = \sum_{j,k=1}^4 \Psi_j J_{ijk} \Psi_k$$

so that the system can be written in compact form as follows:

$$\frac{d\Psi}{dt} + \mathbf{J}\Psi + \mathbf{L}\Psi = \mathbf{W}$$

For all the details and parameter values see Pierini (2011). See also a poster of the same author in session NP3.1.

Coherence resonance



If the model is forced by a time-independent climatological wind stress curl, intrinsic variability emerges, as shown by the bifurcation diagram (left) for $10^{-5} \cdot \Psi_1$ versus a normalized wind amplitude μ ($\mu=1$ corresponds to the homoclinic bifurcation, the dot denotes the first Hopf bifurcation and the thick dashed line the branch of the unstable steady state).

Examples of orbits in the Ψ_1 - Ψ_3 (black) and Ψ_2 - Ψ_4 (gray) planes are shown for local oscillations just before the homoclinic bifurcation ($\mu=0.991$, right-upper panel) and for relaxation oscillations just after it ($\mu=1.043$, right-lower panel).

Let us now force the system with the time-dependent forcing:

$$\frac{d\tau(y, t)}{dy} = -G(t) \frac{d\tau_0(y)}{dy},$$

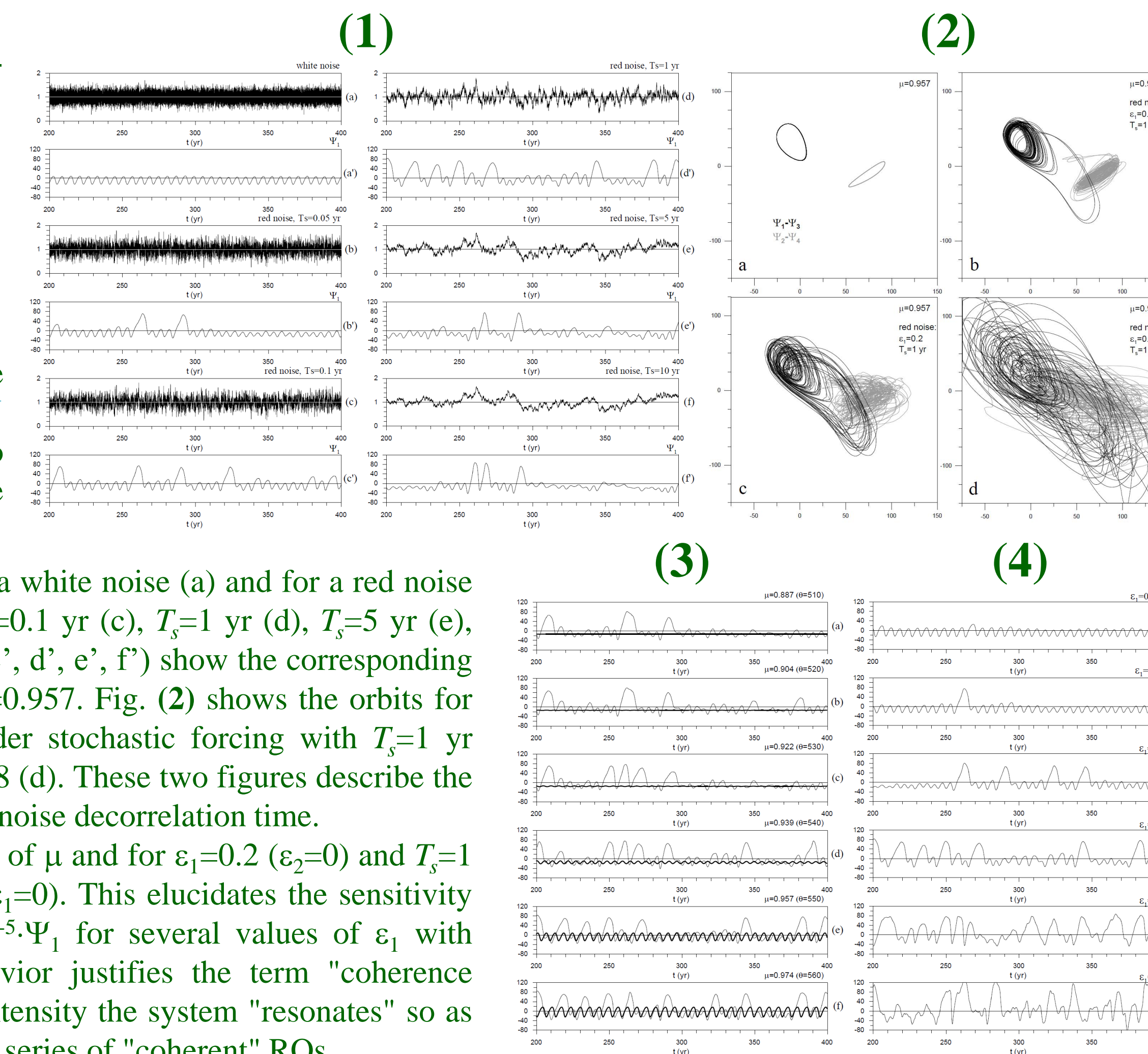
where the temporal coefficient $G(t)$,

$$G(t) = 1 + \varepsilon_1 \frac{\zeta(t)}{\sigma_\zeta} + \varepsilon_2 \sin(\omega t)$$

includes an additive noise solution of the Ornstein-Uhlenbeck equation $\dot{\zeta} = -c\zeta + d\xi$ where ξ is a Gaussian white noise with zero mean and unit variance, c and d are positive constants, and σ_ζ is the r.m.s. of ζ .

Fig. (1) shows G with $\varepsilon_1=0.2$ ($\varepsilon_2=0$) for a white noise (a) and for a red noise with a decorrelation time $T_s=0.05$ yr (b), $T_s=0.1$ yr (c), $T_s=1$ yr (d), $T_s=5$ yr (e), and $T_s=10$ yr (f). In the same figure (a', b', c', d', e', f') show the corresponding model response in terms of $10^{-5} \cdot \Psi_1$ with $\mu=0.957$. Fig. (2) shows the orbits for $\mu=0.957$ under steady forcing (a), and under stochastic forcing with $T_s=1$ yr ($\varepsilon_2=0$) and $\varepsilon_1=0.05$ (b), $\varepsilon_1=0.2$ (c), and $\varepsilon_1=0.8$ (d). These two figures describe the occurrence of CR and its dependence on the noise decorrelation time.

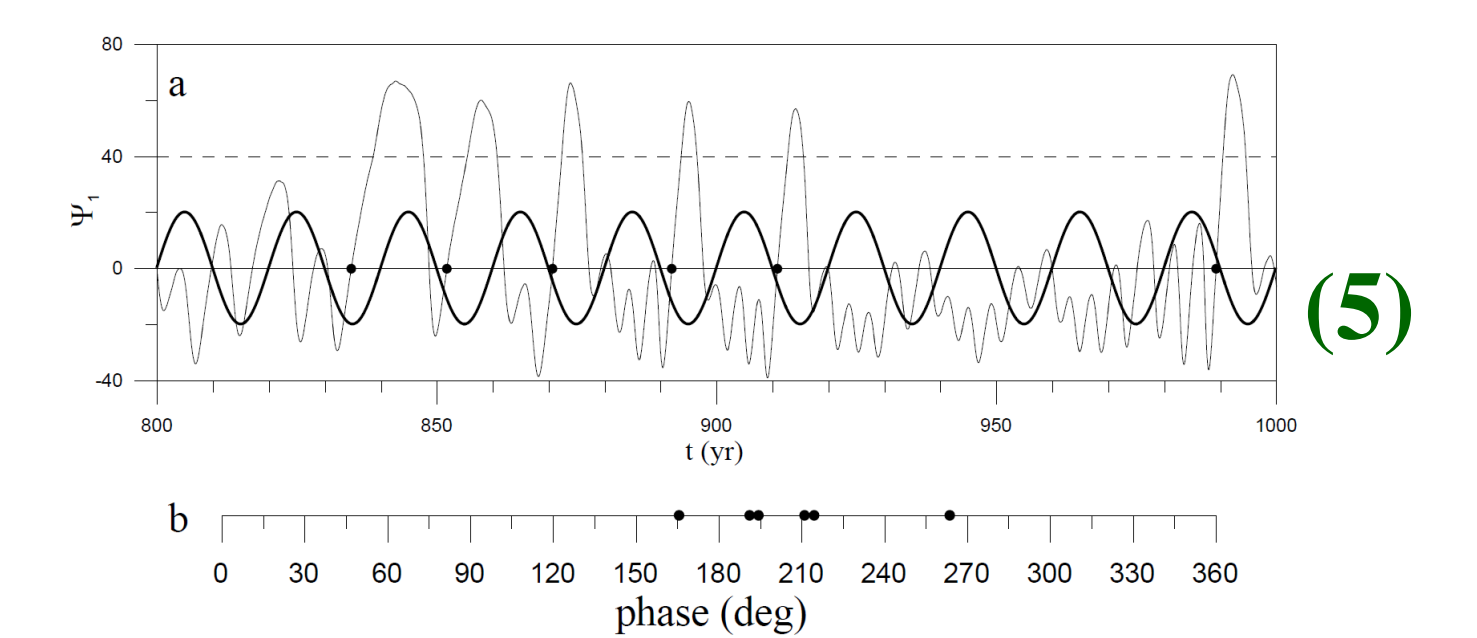
Fig. (3) shows $10^{-5} \cdot \Psi_1$ for several values of μ and for $\varepsilon_1=0.2$ ($\varepsilon_2=0$) and $T_s=1$ yr (the thick lines show the response with $\varepsilon_1=0$). This elucidates the sensitivity of CR to $\mu - \mu_0$. Finally, Fig. (4) shows $10^{-5} \cdot \Psi_1$ for several values of ε_1 with $\mu=0.957$ and $T_s=1$ yr. The resulting behavior justifies the term "coherence resonance": for an optimal range of noise intensity the system "resonates" so as to produce a strong signal characterized by a series of "coherent" ROs.



Phase selection

We have just seen how the occurrence of CR depends in a subtle way both on the decorrelation time and amplitude of the noise forcing. Subtle is also the mechanism that leads to the actual excitation of a single RO. Understanding such mechanism is obviously of crucial importance, as it would provide valuable information on the functioning and predictability of the system.

In order to study this we characterize each RO (conventionally defined here as an oscillation for which the relative maximum $\Psi_{1\max}$ of Ψ_1 is $\Psi_{1\max} > \Phi$ for a given threshold Φ) by means of the time t_z at which Ψ_1 vanishes just before $\Psi_{1\max}$. With $\Phi=40$, the times $t_z(k)$ ($k=1, \dots, N_z=6$) are evidenced by the dots in Fig. (5a) in the case $\mu=0.957$, $\varepsilon_1=0.1$, $T_s=1$ yr plus a fictitious periodic component (thick line) with $\varepsilon_2=0.2$ and $2\pi/\omega=20$ yr:



One can then use the phases $\phi_z(k) = \omega t_z(k) \pmod{2\pi}$ to characterize the excitation. The distribution of the six phases ϕ_z shown in Fig. (5b) yields a clustering around $\phi \approx 200^\circ$, suggesting that those ROs are strongly affected by the phase of the periodic signal (with that particular frequency and amplitude): this is what we mean here by "phase selection" (a weak form of phase locking).

In the figure to the right the relative frequency $v(\phi)$ of occurrence of ϕ_z over 1000-yr-long time series is shown for 16 different forcings. In most cases $v(\phi)$ phase selection is clearly active.

